Quantum Oscillations of Photogalvanic Effect and Spin Orbit Interaction Effect in HgTe Quantum Wells with Parabolic and Dirac Dispersion

C. Zoth,[1] P. Olbrich,[1] K.-M. Dantscher,[1] V.V. Bel'kov,[2] M.A. Semina,[2] M.M. Glazov,[2] L.E. Golub,[2] D.A. Kozlov,[3] Z.D. Kvon,[3] N.N. Mikhailov,[3] S.A. Dvoretsky,[3] and S.D. Ganichev[1]
[1] *Terahertz Center, University of Regensburg, 93040 Regensburg, Germany*
[2] *A.F. Ioffe Physical-Technical Institute, Russian Academy of Sciences, 194021 St. Petersburg, Russia and*
[3] *Institute of Semiconductor Physics, Novosibirsk, Russia*

PACS numbers:

I. INTRODUCTION

II. SAMPLES AND METHODS

The experiments are carried out on (013)-oriented HgTe/$Hg_{0.3}Cd_{0.7}Te$ single QW structures with different widths L_w, of 5 nm, 6.6 nm, 7 nm, 8 nm, 20 nm and 21 nm and with mobilities of about $10^5\,cm^2/(V{\cdot}s)$ at $T = 4.2\,K$[?] . The typical cross section of the structure is shown in Fig.?? (a). In HgTe, an increase of the QW thickness results in the qualitative change of the band structure, starting with a normal parabolic dispersion (5 nm QW), switching to Dirac cones (6.6 nm) and finally changing to a inverted, close to parabolic, band structure (7 nm, 8 nm, 20 nm and 21 nm). The samples with different QW width L_w, are prepared in different geometries including Hall bar and cross shaped structures and squared samples of $5{\times}5\,mm^2$ size, without and with a semitransparent gate. The structures' designs are shown in Fig. ?? (b)-(d). For the square shaped samples eight ohmic contacts have been prepared in the middle of the edges and on the corners, which allow the measurement of voltage drop across the sample. Magnetotransport measurements show well pronounced Shubnikov-De Haas (SdH) oscillations, see Fig. ??, ??, ??, ??, and quantum Hall plateaus (Fig. ??). The gated samples have been used to achieve a controllable variation of the carrier density.

For photocurrent excitation we apply a *cw* CH_3OH laser emitting a radiation with frequency $f = 2.54\,THz$ (wavelength $\lambda = 118\,\mu m$) and $f = 1.62\,THz$ ($\lambda = 184\,\mu m$)[?] . The incident power $P \approx 10\,mW$ is modulated at about 700 Hz by an optical chopper. The radiation at normal incidence is focused in a spot of about 1.5 mm diameter at the center of sample. The spatial beam distribution has an almost Gaussian profile which is measured by a pyroelectric camera[?] ???. The initial linear polarization is transformed into right (σ^+) and left (σ^-) handed circularly polarized light by applying a $\lambda/4$-plate. The magnetic field B up to 7 T is applied normal to the QW plane. Due to the low symmetry of (013)-oriented HgTe QWs, excitation by normally incident THz radiation results in a photogalvanic current even at $B = 0$ T[? ? ?] , for details see[?] . The current-induced photoresponse U are picked up across a 1 MΩ load resistor applying lock-in technique. The photoresponse studies are accompanied by photoconductivity, optical transmission, and magnetotransport experiments.

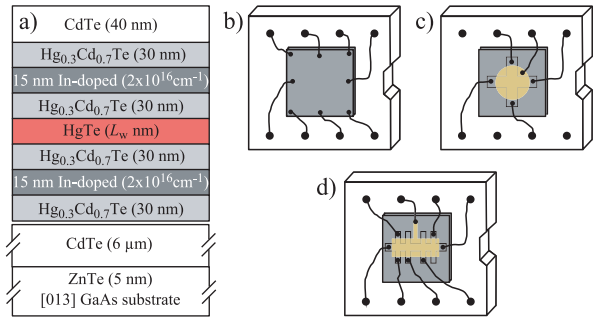

FIG. 1: (a) Cross section of the investigated structures with quantum well width L_W. (b)-(d) show indium contacting of the samples to sample holder for square, cross and Hall bar design, respectively.

III. EXPERIMENTAL RESULTS

We start with the data obtained for the 8 nm Hall bar sample, see Fig. ??. Exciting the sample with linearly polarized radiation and sweeping the external magnetic field we observe that the induced photoresponse is enhanced for magnetic fields larger than 2 T and shows an oscillating behavior (shown in Fig. ??(a)). The envelope of these oscillation behaves Lorentz-like. The observed oscillations perfectly correlate with the SdH oscillations, measured by magnetotransport in the same sample (black dashed line). A similar behavior, with the same Lorentz-like envelope, is observed in the photoconductivity (PC), measured in a biased samples, see Fig. ??(b). These oscillations, however have a phase shift and do not completely follow the SdH frequency. While oscillations for PC with similar features have been reported in HgTe and other low dimensional systems[?] , oscillations in photoresponse are observed for the first time. The Lorentz-like envelope with a maximum at $B = 3$ T indicates that the signal enhancement of both, photoresponse and PC, is due to the cyclotron resonance (CR).

In order to verify the origin of the signal enhancement, we switch to a square shaped sample with the same QW

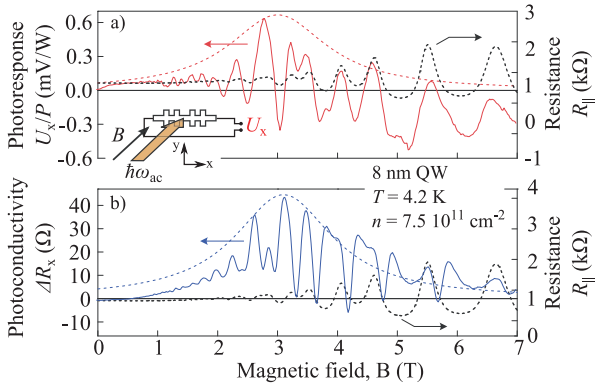

FIG. 2: Photoresponse (a) and photoconductivity (b) as a function on the magnetic field B measured in a ungated 8 nm Hall bar sample excited by linearly polarized radiation. The photoresponse U_x is normalized by radiation power P induced in an unbiased sample and the photoconductivity response ΔR_x is measured for a biased sample. Dashed curves show Lorentzian fit and SdH oscillations of Resistivity $R_{||}$ in color and black, respectively. Inset shows the experimental geometry.

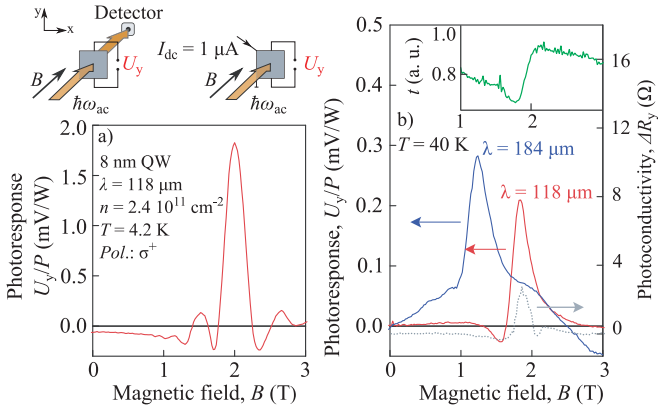

FIG. 3: Photoresponse normalized by radiation power, U_y/P for the 8 nm square sample, excited by σ^+ radiation vs. magnetic field B at (a) $T = 4.2$ K and (b) $T = 40$ K. Latter is shown for two different wavelengths, 118 μm (red curves) and 184 μm (blue curve). In addition, the dotted curve (right scale) presents the change of photoconductivity, ΔR_y, for 118 μm and the inset shows transmission measurement.

thickness $L_w = 8$ nm, which allows us to preform additional measurements of radiation transmission. Studying the photoresponse we also see a oscillating behavior, correlating with SdHs (not shown), and a strong maximum at $B = 2$ T (see Fig. **??**(a)). Increasing the temperature from 4.2 K to 40 K, we observe that the oscillations almost disappear for photoresponse and photoconductivity (Fig. **??**(b), left and right scale, respectively), as well as, for SdHs (not shown). The inset of Fig. **??** (b) shows the transmission measurement, which reveals a pronounce dip whose position fits well to the photoresponse maxima. Furthermore an increment of the radiation wavelength from $\lambda = 118$ μm to $\lambda = 184$ μm resultes in a linear in the wavelength shift of the magnetic field corresponding to the photoresponse maximum. All these observation support the conclusion that the Lorentz-like behavior of the signals' envelope is caused by cyclotron resonance. The lower magnetic field strength of 2 T, at which the Lorentzian envelope shows the maxima (CR position) in the squared sample (Fig. **??**(a)) compared to that in the Hall bar sample (3 T, Fig. **??**(a)), is attributed to the substantial difference in the carrier density by a factor of three and the strong effect of the band nonparabolicity well known for this material**?** .

For studying the effect of electron gas heating at CR absorption, we carried out a detailed study of the photoconductivity, measured by two different methods applied to the 8 nm square shaped sample. The data are shown in Fig. **??**(b)-(d). Photocurrent data, obtained for the same sample, is shown for comparison (Fig. **??**(a)). As a first method we used a *dc* bias voltage of $\pm$ 1 V, a pre-resistor of 1 MΩ ($I_{dc} = \pm$ 1 μA through sample) and modulated the radiation (Fig. **??** b). The induced change of resistance ΔR shows a resonance and oscillating behavior upon variation of the magnetic field strength. In the second method we measured the SdH oscillations and Hall effect, via standard magnetotransport measurement, in the dark and in the presence of unmodulated THz radiation (Fig. **??** (c)). While the period of the oscillation does not change in the range of the CR (≈ 2 T), we do see a substantial change in the sample resistance caused by the electron gas heating and a corresponding reduction of the electron mobility. The difference between the dashed and solid lines of Fig. **??** (c) (PC signal) is shown in panel (d) as a solid line. Comparison of Figs. (a), (b) and (d) shows that they are in a good agreement and that the oscillating behavior correlates well with the SdH oscillations shown in (c). Furthermore a simple theoretical approach of fitting the PC data was done here. Therefore the standard SdH curve (Fig. **??**(c), dashed line), measured at $T = 4.2$ K, has been fitted by standard expression**?** and by taking into account Lorentzian-like electron gas heating with effective temperature $T_{eff} = 13.9$ K at a CR position of approximately 2 T. Calculating the difference for these two SdH fit functions, we obtain the dotted line presented in Fig. **??**(d), which is in good accordance with real measured PC (solid line).

Similar results are observed for other samples with inverted and non-inverted parabolic dispersion, see Fig. **??** (a)-(c). All samples show an oscillating behavior at $T = 4.2$ K which is reduced to a single peak when increasing the temperature.

We now consider a 20 nm QW cross shaped sample with a semitransparent gate. The results on photoresponse can be seen in Fig. **??**. The above addressed dependence of the magnetic field, at which the photoresponse peak emerges, on the carrier density can be confirmed here. Fig. **??** (c) shows, that by tuning the carrier density with gate voltage U_g from 0 to 4 V, the resonance position of the signal shifts from $B = 3.06$ to 2.88 T. This is attributed to the moderate density dependence of the

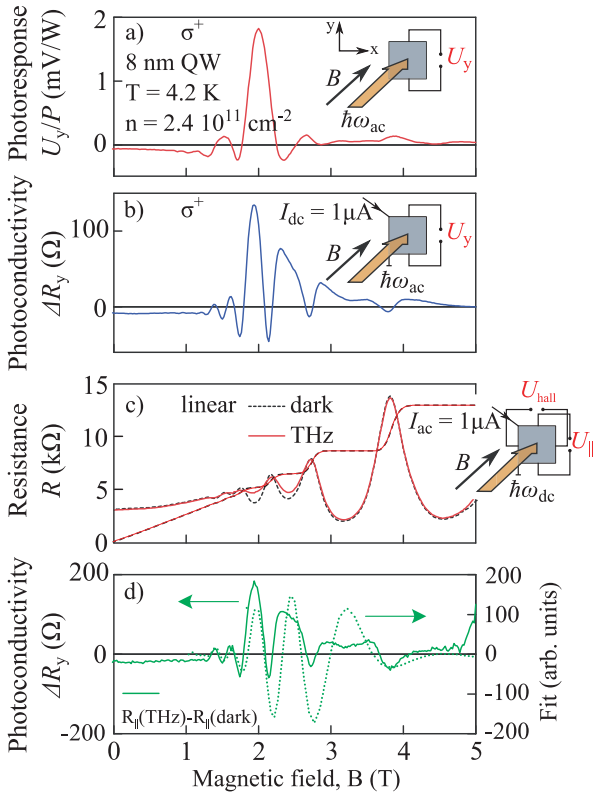

FIG. 4: Measurements for the 8 nm square sample $T = 4.2$ K. (a) Photoresponse normalized by radiation power U_y/P. (b) Change of photoconductivity, ΔR_y, for *dc* bias and modulated radiation (first method). (c) Magnetotransport measurement of Shubnikov-De Haas oscillations, with and without *dc* radiation, solid and dashed line, respectively. (d) ΔR_y for *ac* bias and *dc* radiation (second method, left scale) and theoretical fit (right scale).

cyclotron resonance mass due to the band nonparabolicity. Fixing the magnetic field $B = 2.96$ T at a value close to CR condition for all densities, we measured the photoresponse as a function of the electron density and observed SdH oscillation also is this type of experiments (see Fig. **??**(b)). A density increase, for large U_g, causes the signal to grow in magnitude.

Similar measurements were also done on a Dirac fermion system, a gated 6.6 nm Hall bar sample, which is characterized by a linear energy spectra[? ?] . Oscillations at fixed magnetic field values B 0 1.5 and 2 T as a function of the gate voltage are observed and shown in Fig. **??** (a) and (b). Here we have a good correlation of photoresponse (left scale) and SdH (right scale) oscillations and an envelope with a clear maximum. The latter is even more pronounced for smaller magnetic field. The strong dependence of the envelope maximum on the carrier density n results from the Dirac dispersion of the charge carriers in this sample. The CR position varies with the carrier density as $n \propto \sqrt{B}$. Fig. **??** (c) shows the resonant magnetic field B^{CR} as a function of the carrier density with a fit of $n \propto \sqrt{B}$, which describes our data well.

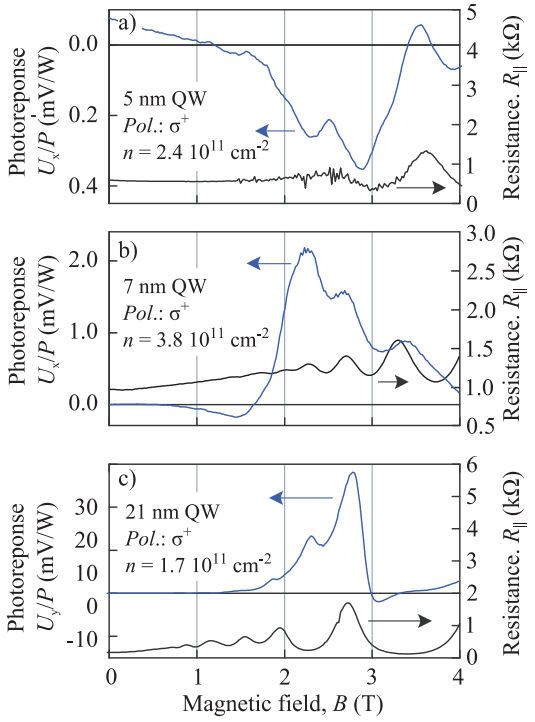

FIG. 5: Photoresponse normalized by radiation power $U_{x,y}/P$ (left scale) and SdH oscillations (right scale) for three different QW widths, (a) $L_w = 5$ nm, (b) $L_w = 8$ nm and (c) $L_w = 21$ nm.

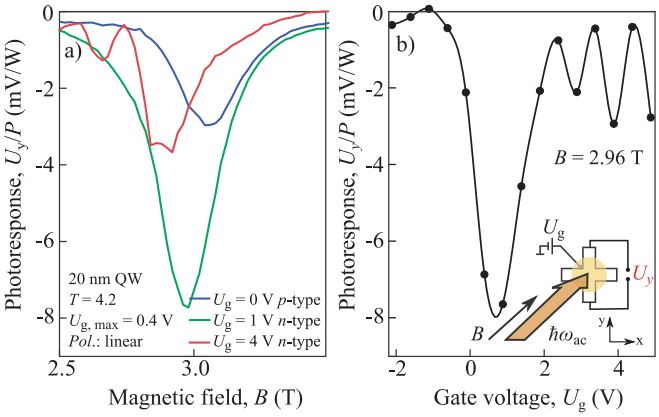

FIG. 6: Normalized photoresponse U_y/P for the gated cross shaped 20 nm QW sample (a) as a function of the magnetic field B for fixed gate voltages $U_g = 0$, 1 and 4 V and (b) vs. the gate voltage U_g for fixed magnetic field $B = 2.56$ T.

To conclude the experimental part we observed SdH oscillations in photoresponse and in the change of photoconductivity for normal and inverted parabolic dispersion, as well as, for Dirac fermions. The oscillations are enhanced at cyclotron resonance position and vanish with increasing the temperature, showing only one sharp peak in signal due to CR.

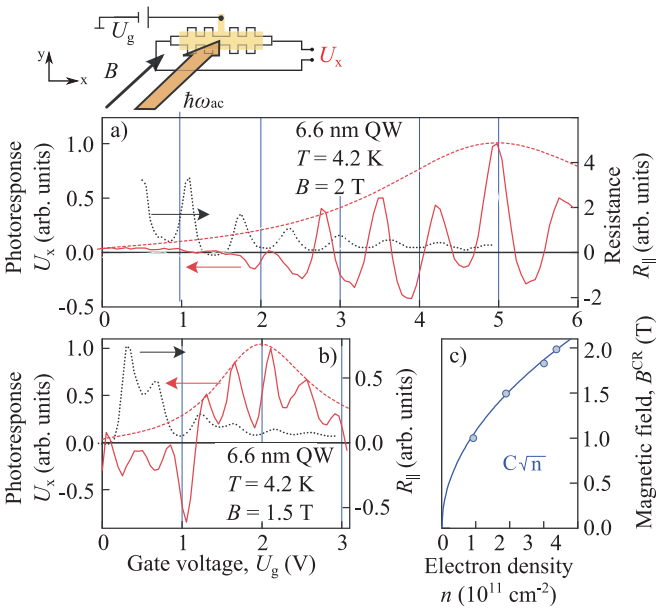

FIG. 7: (a) and (b) show normalized photoresponse (left scale) and SdH oscillations (right scale) depending on the gate voltage U_g for two different magnetic field values, 2 and 1.5 T, respectivly. The dashed lines correspond to Lorentz-like envelope functions indicating a resonance-like behavior. (c) Value of the magnetic field at the maximum of photoresponse U_x as a function of electron density, showing a $\propto C\sqrt{n}$ dependence.

[1] Thesis, papers, Krishtopenko + works of Nijnii Novgorod
[2] Z.D. Kvon, E.B. Olshanetsky, N.N. Mikhailov, and D.A. Kozlov, Low. Temp. Phys **35**, 6 (2009).
[3] J. R. Meyer, C.A. Hoffman, F.J. Bartoli, T. Wojtowicz, M. Dobrowolska, J.K Furdyna, X. Chu, J.P. Faurie, and L.R. Ram-Mohan, J. Vac. Sci. Technol. **B10**, 1582 (1992).
[4] B. Wittmann, S.N. Danilov, V.V. Bel'kov, S.A. Tarasenko, E.G. Novik, H. Buhmann, C. Brüne, L.W. Molenkamp, E.L. Ivchenko, Z.D. Kvon, N.N. Mikhailov, S.A. Dvoretsky, N.Q. Vinh, A.F.G. van der Meer, B. Murdin, and S.D. Ganichev, Semicond. Sci. Technol. **25**, 095005 (2010).
[5] E. Ziemann, S.D. Ganichev, I.N. Yassievich, V.I. Perel, and W. Prettl, J. Appl. Phys. **87**, 3843 (2000).
[6] Z. D. Kvon, S.N. Danilov, N.N. Mikhailov, S.A. Dvoretski, and S.D. Ganichev, Physica E **40**, 1885 (2008).
[7] M. von Truchsess, V. Latussek, C.R. Becker, and E. Batke, J. Cryst. Growth **159**, 1104 (1996).
[8] V.J. Goldmann, H.D. Drew, M. Shayegan, and D.A. Nelson, Phys. Rev. Lett. **56**, 968 (1986).
[9] M.I. D'yakonov, and A.V. Khaetskii, ????, ??? (1981).
[10] K.-J. Friedland, R. Hey, H. Kostial, R. Klann, and K. Ploog, Phys. Rev. Lett. **77**, 4616 (1996).
[11] C. Notthoff, K. Rachor, D. Heitmann, and A. Lorke, Phys. Rev. B **80**, 205320 (2009).
[12] M. Zholudev, M. Orlita, C. Consejo, J. Torres, N. Dyakonova, M. Czapkiewicz, J. Wrbel, G. Grabecki, N. Mikhailov, S. Dvoretskii, A. Ikonnikov, K. Spirin, V. Aleshkin, V. Gavrilenko, and W. Knap, Phys. Rev. B **86**, 205420 (2012).
[13] M. Schultz, F. Heinrichs, U. Merkt, T. Colin, T. Skauli, and S. Løvold, Semicond. Sci. Technol. **11**, 1168 (1996).
[14] M. Schultz, U. Merkt, A. Sonntag, U. Rössler, T. Colin, P. Helgesen, T. Skauli, and S. Løvold, J. Cryst. Growth **18485**, 1180 (1998).
[15] M. Schultz, U. Merkt, A. Sonntag, U. Rössler, R. Winkler, T. Colin, P. Helgesen, T. Skauli, and S. Løvold, Phys. Rev. B **57**, 14772 (1998).
[16] S.Y. Liu, and X.L. Lei, J. Phys. Cond. Mat. **15**, 4411 (2003).
[17] X.L. Lei, and S.Y. Liu, Appl. Phys. Lett. **82**, 3904 (2003).
[18] O.E. Raichev, Phys. Rev. B **85**, 045310 (2012).
[19] B.N. Murdin, A.R. Hollingworth, M. Kamal-Saadie, R.T. Kotitschke, C.M. Ciesla, C.R. Pidgeon, P.C. Findlay, H.P.M. Pellemans, C.J.G.M. Langerak, A.C. Rowe, R.A. Stradling, and E. Gornik, Phys. Rev. B **59**, R7817 (1999).
[20] V.G. Golubev, V.I. Ivanov-Omskii, and G.I. Kropotov, Sov. Tech. Phys. Lett. **3**, 216 (1978).
[21] C.-M. Hu, C. Zehnder, C. Heyn, and D. Heitmann, ??? **???**, ??? (????).
[22] K.C. Nowack, E.M. Spantor, M. Baenninger, M. König, J.R. Kirtley, B. Kalisky, C. Ames, P. Leubner, C. Br"*u*ne, H. Buhmann, L.W. Molenkamp, D. Goldhaber-Gordon, and K.A. Moler, Nature Mater. **???**, ??? (2013).
[23] M. S. König, S. Wiedmann, C. Brüne, A. Roth, H. Buhmann, L. Molenkamp, X. L. Qi, and S. C. Zhang, Science **318**, 766 (2007).
[24] B. A. Bernevig, T. L. Hughes, and S. C. Zhang, Science

314, 1757 (2006).
[25] B. Büttner, C. X. Liu, G. Tkachov, E. G. Novik, C. Brüne, H. Buhmann, E. M. Hankiewicz, P. Recher, B. Trauzettel, S. C. Zhang, and L.W. Molenkamp, Nature Phys. **7**, 418 (2011).
[26] Z. D. Kvon, S.N. Danilov, D.A. Kozlov, C. Zoth, N.N. Mikhailov, S.A. Dvoretskii, and S.D. Ganichev, JETP Lett. **94**, 816 (2011).
[27] P. Olbrich, C. Zoth, P. Vierling, K.-M. Dantscher, G. V. Budkin, S. A. Tarasenko, V. V. Bel'kov, D. A. Kozlov, Z. D. Kvon, N. N. Mikhailov, S. A. Dvoretsky, and S. D. Ganichev, Phys. Rev. B **87**, 235439 (2013).
[28] J. Schliemann, New J. Phys. **10**, 043024 (2008).
[29] E.M. Lifshitz, L.P. Pitaevskii, *Physical Kinetics*, Butterworth-Heinemann, Oxford (1981).
[30] X.C. Zhang, K. Ortner, A. Pfeuffer-Jeschke, C.R. Becker, and G. Landwehr, Phys. Rev. **(**69), 115340 (2004).
[31] S. D. Ganichev, E. L. Ivchenko, and W. Prettl, Physica E **14**, 166 (2002).
[32] P. Schneider, J. Kainz, S.D. Ganichev, V.V. Bel'kov, S.N. Danilov, M.M. Glazov, L.E. Golub, U. Rssler, W. Wegscheider, D. Weiss, D. Schuh, and W. Prettl, J. Appl. Phys. **96**, 420 (2004).
[33] S. D. Ganichev and W. Prettl, *Intense Terahertz Excitation of Semiconductors* (Oxford Univ. Press, 2006).
[34] E. L. Ivchenko, *Optical Spectroscopy of Semiconductor Nanostructures* (Alpha Science, 2005).
[35] S. D. Ganichev, *et al.*, Nature Phys. **2**, 609 (2006).
[36] V. V. Bel'kov, and S. D. Ganichev, Semicond. Sci. Technol. **23**, 114003 (2008).
[37] S.D. Ganichev *et al.*, Phys. Rev. Lett. **102**, 156602 (2009).
[38] P. Olbrich *et al.*, Phys. Rev. B **85**, 085310 (2012).
[39] *Spin Physics in Semiconductors*, ed. M.I. Dyakonov (Springer, 2008).
[40] (013)-grown QWs belong to the C_1 point group. Thus, the coupling between the components of $\boldsymbol{k}$ and spin vector is not predefined by symmetry.